Supporting Information

Controlled assembly of hybrid architectures based on carboxylic acid ligand and $[(O_3PCH_2PO_3)Mo_6O_{22}]^{12-}$

Xiaopeng Sun, Donghui Yang, Gaigai Wang, Zhijie Liang, Pengtao Ma, Jingping Wang* and Jingyang Niu*

Key Laboratory of Polyoxometalate Chemistry of Henan Province,
Institute of Molecular and Crystal Engineering,
College of Chemistry and Chemical Engineering,
Henan University, Kaifeng 475004, Henan, China,
E-mail: jpwang@henu.edu.cn, jyniu@henu.edu.cn; Fax: (+86)371-23886876.

CONTENTS

Section1. IR spectra of 1−3 and carboxylic acid ligands

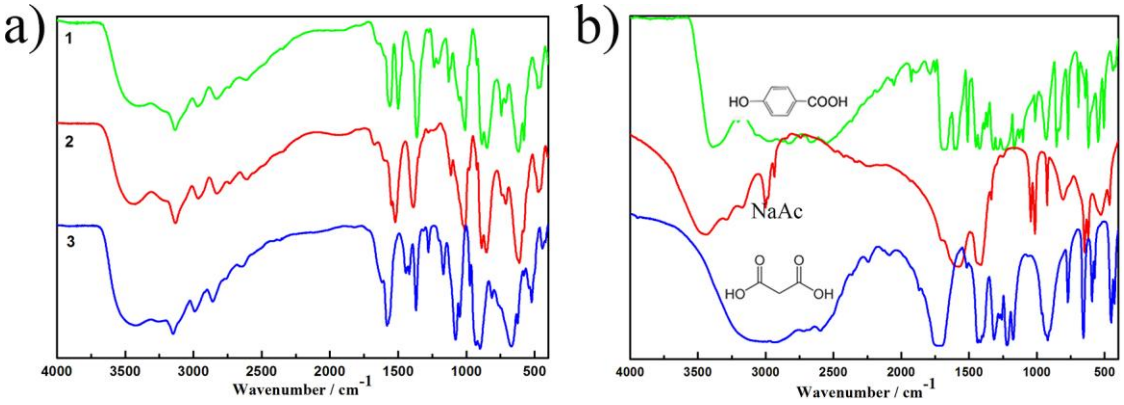

Fig. S1 (a) IR spectra of **1–3**; (b) IR spectra of p-hydroxybenzoic acid, NaAc and malonic acid

Section2. The comparison of experimental XRPD patterns (in red) and simulated (in black) of 1−3

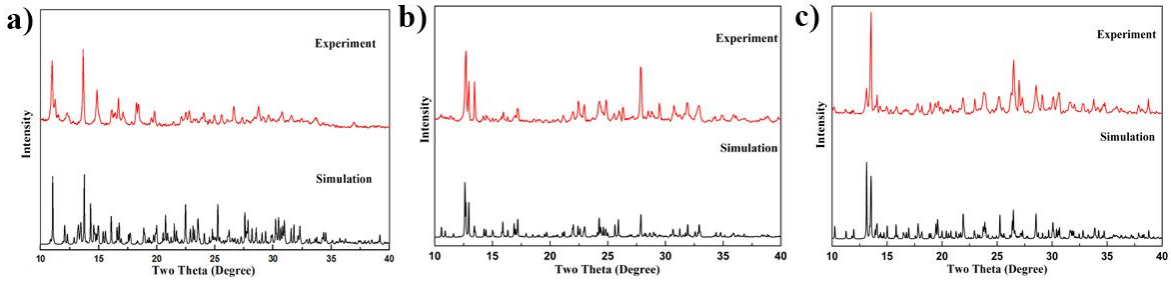

Fig. S2 The Comparison of simulated (in black) and experimental XRPD patterns (in red) of **1−3**

The comparison of the simulated and experimental XRPD patterns for **1**, **2** and **3** are shown in Fig.S2a, S2b and S2c, respectively. Their peak positions are in good agreement with each other, indicating the phase purity of the products. The differences in intensity may be due to the preferred orientation of the powder samples.

Section3. The UV-vis spectra of 1−3

The UV-vis spectra of **1−3** are performed in the aqueous solution at ambient temperature. The UV-vis spectra display one strong absorption band centered at 206 nm which is assigned to the pπ-dπ charge transfer transitions from O_t→Mo. The wide shoulder absorption band centered at ca. 247 nm of **1** is attributed to $O_{b,c}$→Mo charge transfer transitions.[S1]

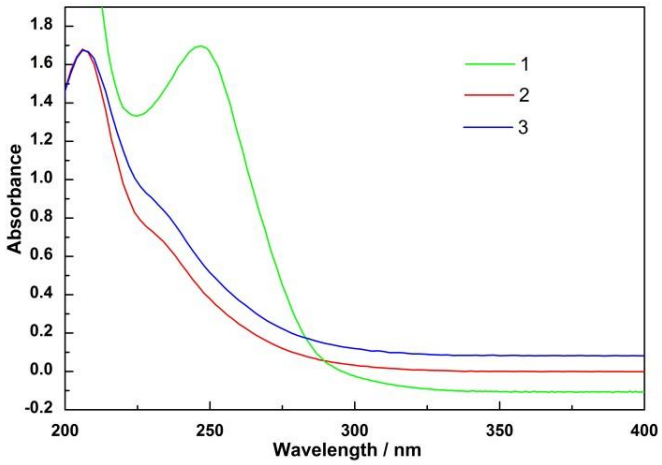

Fig. S3 UV-vis spectra of **1−3**.

Section4. ^{31}P NMR spectroscopic characterization of 1−3 with time and $H_2O_3PCH_2PO_3H_2$

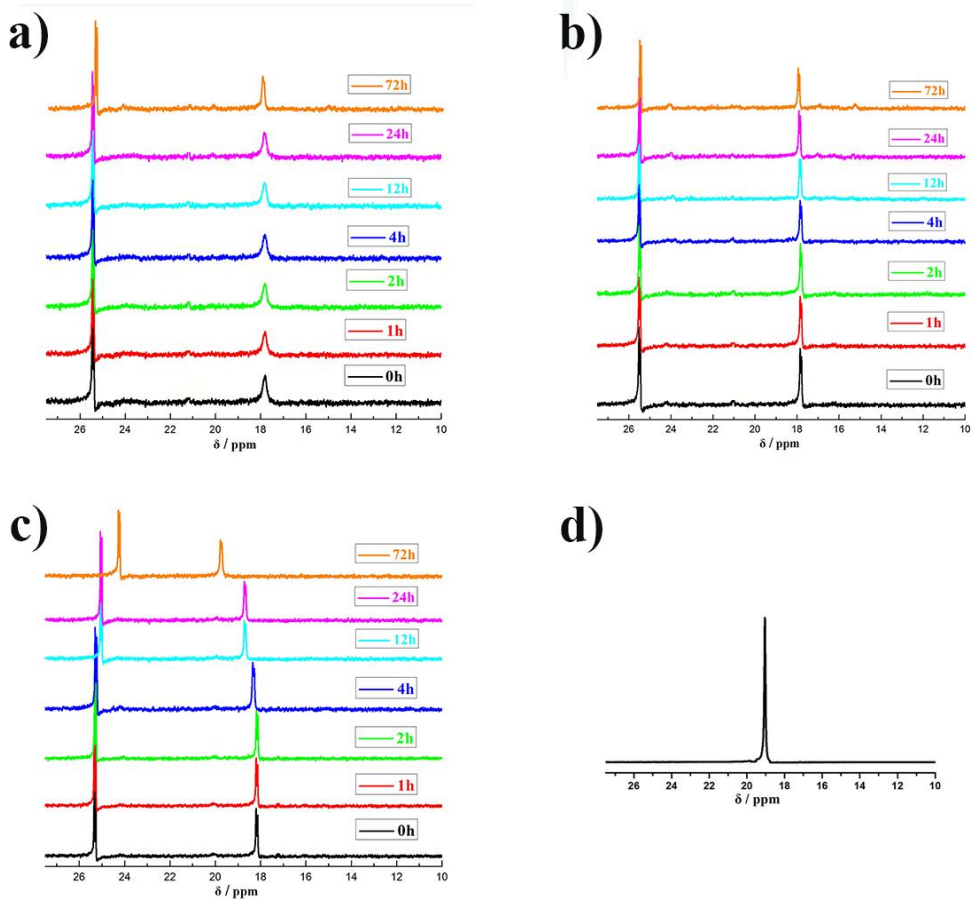

Fig. S4 ^{31}P NMR spectra of **1** (a), **2** (b) and **3** (c) with time dissolved in D_2O at room temperature; ^{31}P NMR spectrum of $H_2O_3PCH_2PO_3H_2$ (d) dissolved in D_2O at room temperature.

Section5. Thermogravimetric analyses of 1−3

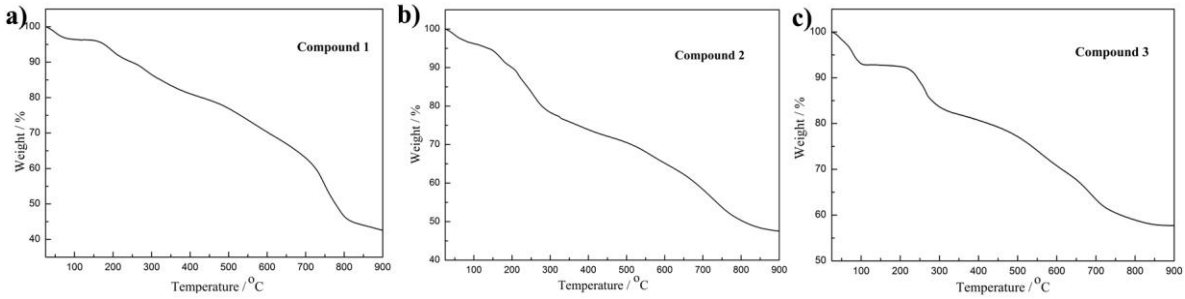

Fig. S5 Thermogravimetric analysis curve of **1**−**3**.

To investigate the thermal stabilities of **1**–**3**, thermal gravimetric (TG) analyses were performed under a nitrogen flow in the range of 25–900 ℃. The TG curve of **1** shows two slow steps of weight loss in the temperature range 25–900 ℃ (Fig. S5a). The weight loss of 4.43 % from 25 to 168 ℃ is ascribed to the escaping of nine point five crystalline water molecules (calc. 9.25 %). The residual weight loss at this temperature range is high that expected for the stoichiometric amount, which probably because these crystals easily lost crystalline water molecules in the air. The second step of weight loss is 53.01% at 168–900 ℃, which is attributed to the loss of one $H_2O_3PCH_2PO_3H_2$ molecule, two p-hydroxybenzoic acid molecules, five $C_3H_4N_2$ molecules and the sublimation of metal oxides. [S2]

For **2** (Fig.S5b), the first step of weight loss is 5.58 % from 25 to 150 ℃, which is assigned to the removal of eight crystalline water molecules (calc. 4.67 %). The rest weight loss of 46.86 % in the temperature range 150–900 ℃ is corresponding to the decomposition of POM framework and the release of eight $C_3H_4N_2$ molecules, two $H_2O_3PCH_2PO_3H_2$ molecules, four acetic acid molecules, two structure water molecules and the sublimation of metal oxides.

The thermal decomposition process of **3** is approximately divided into three steps (Fig. S5c). The first weight loss of 7.40% from 25 to 180 ℃ is comparable with the calculated value of 6.61%, corresponding to the loss of fourteen crystalline water molecules. The second step, which occurs from 180 to 490 ℃, is attributed to the loss of eight $C_3H_4N_2$ molecules, and the observed weight loss (14.99%) is in agreement with the calculated value (14.27%).The third stage is attributed to the release of two malonic acid molecules, two $H_2O_3PCH_2PO_3H_2$ molecules and the sublimation of metal oxides., and the observed weight loss of 19.90% can compare with the calculated value of 18.69% from 490 to 900 ℃.

Section6. Bond valence sum calculations of Mo, P and O atoms on POM fragments in 1−3

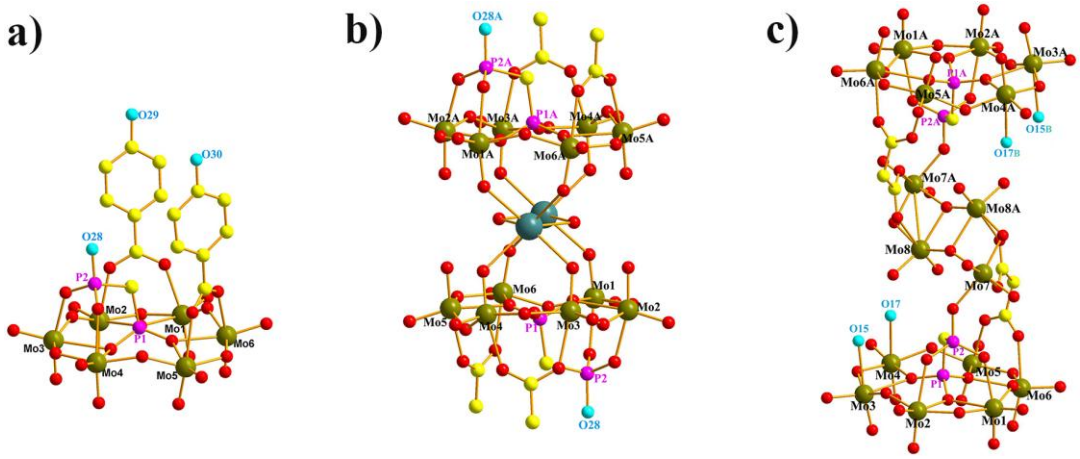

Fig. S6 The representation of Mo, P and O atoms labeling of **1a**−**3a (**The protonized O atoms with sky blue color).

Table S1 Bond valence sum parameters for Mo atoms and P atoms on POM fragments in **1**−**3**.

P/Mo / compound	Mo1	Mo2	Mo3	Mo4	Mo5	Mo6	Mo7	Mo8	P1	P2
Compound **1**	6.213	6.241	6.266	6.272	6.222	6.220	−	−	2.503	2.569
Compound **2**	6.044	6.065	6.067	6.104	6.138	6.082	−	−	2.355	2.470
Compound **3**	6.059	6.069	6.131	6.060	6.101	6.156	6.060	6.098	2.453	2.455

Table S2 The bond valence sum calculations of the oxygen atoms in **1a**.

Atom	Bond valence sum	Atom	Bond valence sum	Atom	Bond valence sum
O1	1.819	O2	1.832	O3	1.918
O4	1.930	O5	1.728	O6	1.921
O7	1.737	O8	1.951	O9	2.057
O10	1.737	O11	1.854	O12	1.921
O13	1.710	O14	1.817	O15	1.779
O16	1.767	O17	2.118	O18	1.769
O19	1.766	O20	1.714	O21	1.947
O22	1.934	O23	1.804	O24	1.878
O25	1.874	O26	1.727	O27	1.701
O28	1.356	O29	1.162	O30	1.123

Table S3 The bond valence sum calculations of the oxygen atoms in **2a**.

Atom	Bond valence sum	Atom	Bond valence sum	Atom	Bond valence sum	Atom	Bond valence sum
O1	1.732	O2	1.842	O3	1.672	O4	1.644
O5	2.065	O6	1.797	O7	1.732	O8	1.697
O9	1.978	O10	1.719	O11	1.715	O12	1.691
O13	1.853	O14	1.879	O15	1.893	O16	1.735
O17	1.708	O18	1.848	O19	1.962	O20	1.729
O21	1.797	O22	1.811	O23	1.878	O24	1.829
O25	1.742	O26	1.881	O27	1.691	O28	1.241

Table S4 The bond valence sum calculations of the oxygen atoms in **3a.**

Atom	Bond valence sum	Atom	Bond valence sum	Atom	Bond valence sum	Atom	Bond valence sum
O1	1.751	O2	1.727	O3	1.732	O4	1.941
O5	2.122	O6	1.832	O7	1.712	O8	1.742
O9	2.046	O10	1.604	O11	1.770	O12	1.740
O13	1.870	O14	1.908	O15	0.242	O16	1.759
O17	0.266	O18	1.767	O19	1.973	O20	1.688
O21	1.697	O22	2.005	O23	1.899	O24	1.760
O25	2.015	O26	1.790	O27	1.721	O28	1.945
O29	1.774	O30	1.783	O31	1.936	O32	1.858
O33	1.997	O34	1.730	O35	2.025	O36	1.840

Section7. The coordination environment of P1 and P2 atoms in 1−3

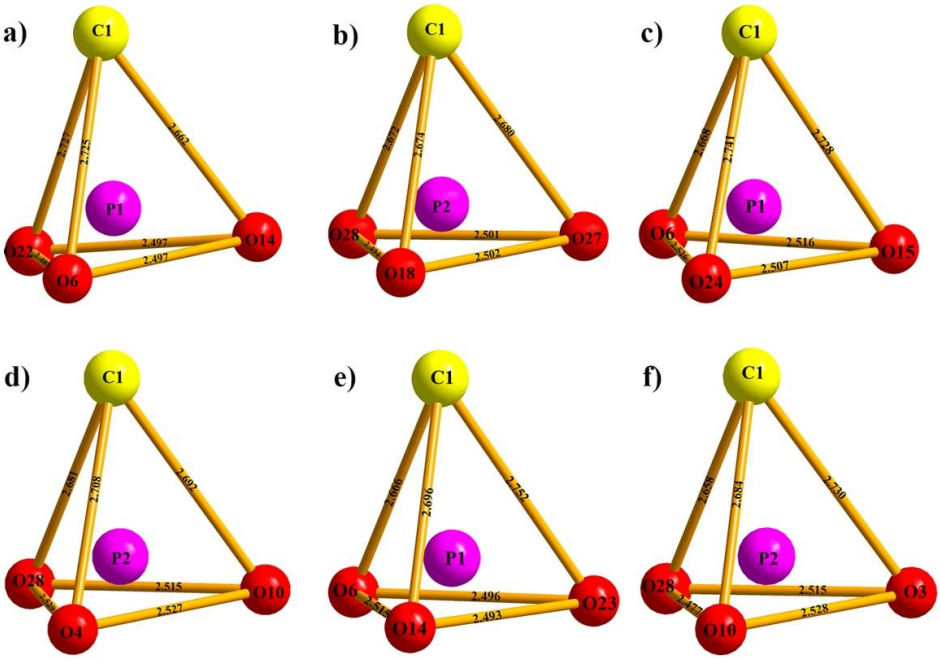

Fig. S7 The coordination environment of P1 and P2. (a and b for **1**; c and d for **2**; e and f for **3**).

Section8. Some other supporting figures

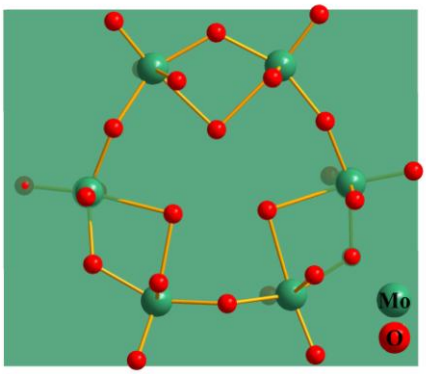

Fig. S8 The structure representation of {Mo_6} plane. (color code: sea green)

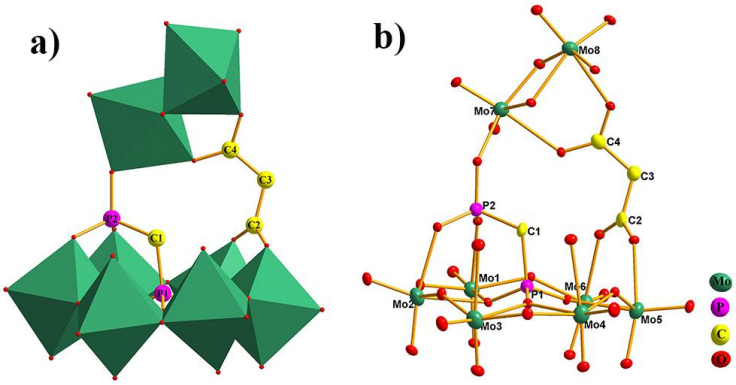

Fig. S9 The structure representation of {($O_3PCH_2PO_3$)($Mo_6O_{18}(H_2O)_2$)($O_2CCH_2CO_2$)(Mo_2O_7)} segment. (Hydrogen atoms are omitted for clarity)

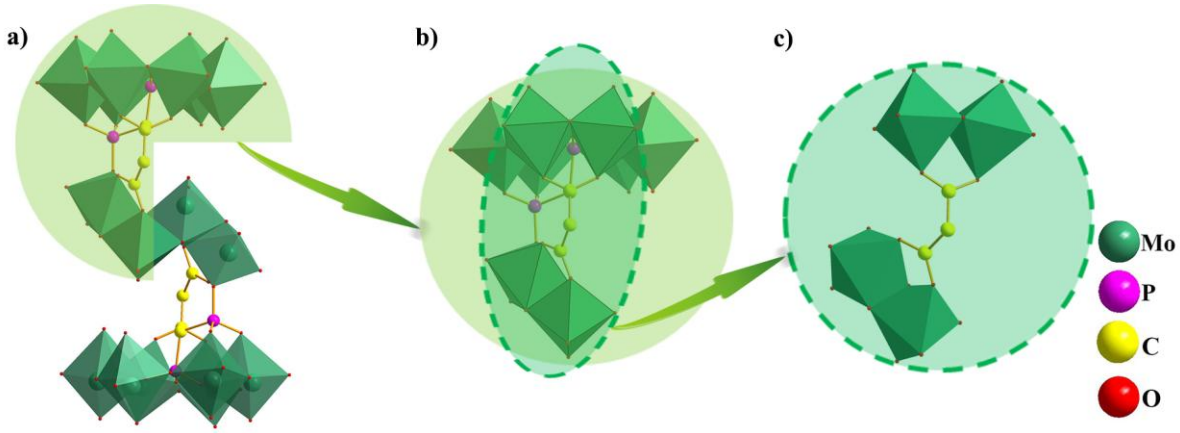

Fig. S10 The bonding way of the two {COO} groups from malonic acid in **3a**.

Table S5 A summary table of the reaction conditions

("√": feasible; "×": unfeasible)

Factor	Condition	Result
Counterion	$[C_3N_2H_5]^+$	√
	K^+	×
molar ratio of Mo/P	<10/3	×
	=10/3	√
	>10/3	×
Temperature	<60 ℃	×
	60 ℃−80 ℃	√
	>80 ℃	×
pH	<3.5	×
	3.5 −5.5	√
	>5.5	×

Section9. References

[S1] J. Y. Niu, J. A. Hua, X. Ma and J. P. Wang, *CrystEngComm.*, 2012, **14**, 4060.

[S2] L. Raki and C. Detellier, *Chem. Commun.*, 1996, 2475.